Turkish Journal of Electrical Engineering & Computer Sciences

http://journals.tubitak.gov.tr/elektrik/

Research Article

Turk J Elec Eng & Comp Sci
(2021) 29: 3119 – 3132

doi:10.3906/elk-2103-108

Evaluation of cable and busbar system in multiconductor distribution systems in terms of current and magnetic field distributions

Yunus Berat Demirol[1], Mehmet Aytaç Çınar[2,*], Bora Alboyacı[3]
[1]GENETEK Güç&Enerji Ltd. Şti, Kocaeli, Turkey
[2]İzmit Vocational School, Kocaeli University, Kocaeli, Turkey
[3]Electrical engineering department, Engineering Faculty, Kocaeli University, Kocaeli, Turkey

Received: 23.03.2021 • **Accepted/Published Online:** 02.07.2021 • **Final Version:** 30.11.2021

Abstract: The selection of power distribution components is of great importance in electrical facilities. Cable and busbar systems are widely used applications, such as electric vehicle charge stations, microgrids and energy storage systems, for power distribution in the distribution grid. In this study, the current distribution on the parallel conductors and magnetic field distributions around cable and busbar structures is evaluated for studied application where the power is distributed using a cable system between a converter transformer and a converter. All modeling and analyzes are conducted using ANSYS Electronics Suite software, by applying balanced and pure sinusoidal current excitation. Obtained results show that, when the busbar system is installed for power distribution, current distribution between parallel conductors is decreased to the negligible level, and the calculated magnetic field density is about 73.7% lower than the cable system.

Key words: Busbar, cable, current distribution, magnetic field, skin effect, proximity effect

1. Introduction

Cable and busbar systems are widely used in the distribution of electrical energy at low voltage levels to the end user. Depending on the application, these systems have pros and cons compared to each other. Especially, in distribution systems where high current values are carried by using many parallel cables together, various electrical and physical problems occur. Some of these problems are given as follows: the decrease in the current carrying capacity of cables installed in parallel as explained in IEC 60364-5-52 standard [1], additional power losses caused by skin and proximity effect, unbalanced loading of cables with respect to each other, magnetic field pollution around the system, difficulty of connecting cable terminals and necessity of the adjustment of most effective phase sequence can be given.

Among these negative aspects of systems with many parallel cables, especially the unbalanced loading of the cables is important for an efficient operation and sustainability of the system. The current distribution on the conductors in parallel cable systems may differ depending on the number and sequence of parallel phases, the layout of the cables, the distance between the cables and the grounding condition of the shield and armor of the cable used. Some of these negative features, which occur in cable systems, can be minimized by using busbar structures. Considering these negativities, detailed analyzes at the design stage of the systems provide advantages in terms of operability and sustainability of the enterprises.

In literature, there are many studies, which investigate the current distributions on the conductors in systems with many parallel cables, and the phase sequences are examined to reduce the imbalance [2–4]. In

*Correspondence: aytac@kocaeli.edu.tr

these studies, three-phase, three and four-wire cable layouts were examined, and current imbalances of up to 119% were determined depending on the number of parallel cables per phase and cable layout. In addition, the temperature levels of cables in parallel cable systems [5], current distributions in cables in the case of loading with harmonic currents [6], phase sequence configurations for reducing magnetic fields in cable systems [7] and calculation of current distributions using finite element method [8] are investigated. In the studies carried out, it has been observed that the current imbalance between the conductors increase up to 263% depending on the number of parallel cables per phase and frequency, especially operating in harmonic current conditions.

Renewable energy (wind, solar, etc.) systems are one of the application areas that are faced with an unbalanced load situation in parallel cables. In these systems, the increase of the converter power results in an increase in the number of parallel cables required on the low voltage side of the transformers to which they are connected. At this point, busbar systems are an important alternatives to reduce the negative effects of currents with high frequency harmonic components.

Busbar systems offer lower electrical voltage drop and higher short-circuit strength characteristics when compared to cable distribution systems. In addition, owing to its metal body, they have high mechanical strength, high IP protection degree and cooling capacity. In literature, there are numerous studies where short circuit simulations are carried out [9, 10], temperature changes are examined by both simulation and experimental methods [11, 12], power losses [13] and thermal and electrodynamic forces are calculated [14] for busbar systems. However, it is observed that studies, which are comparing busbar and cable systems in terms of electrical parameters, are very limited.

In this study, it is aimed to determine the electrical performance of busbar systems and to evaluate their applicability for an application where high current values are carried with parallel cable systems. For this purpose, the current distributions on the conductors and the magnetic field intensities around the distribution systems are compared by means of electromagnetic analyses for both cable and busbar structures for the application under study. The investigated application was modeled in 1:1 scale and analyzed using ANSYS Electronics Suite software. Obtained results were compared and commented in detail.

In this context, economic criteria is another parameter that determines the feasibility of cable and busbar structures. In an economic analysis to be made for this purpose, in addition to the costs of the cable/busbar elements, the labor costs in the installation process and the additional costs related to the operating period should be taken into consideration. Due to the length of the distribution system to be established, the architectural structure in the environment, where the distribution system to be installed, the protection class, environmental effects and other similar parameters must be taken into account. The content of the economic analysis is not included in this study.

2. Calculation of current and magnetic field distributions

In alternating current carrying conductor systems, the skin and proximity effects have a significant role on the current distribution between the conductors. The skin effect causes the increase in the current density in regions close to the conductor surface. However, the proximity effect causes disruption in homogeneity of current distribution in the conductor, depending on the phase sequence and the position of the conductor with other conductors.

Considering the basic conductor system, which consists only two single core cables, alternating current resistance and related coefficients are calculated as given below. The resistance value of a conductor in alternating current is expressed as the sum of the resistance value of this conductor in direct current and

the resistance values due to skin and proximity effect, as given in Eq. (1).

$$R_{ac} = R_{dc} \,.(1 + \ y_s + y_p) \tag{1}$$

Here; R_{ac}, R_{dc}, y_s and y_p are alternating current resistance, direct current resistance, skin effect coefficient and proximity effect coefficient, respectively. Direct current resistance of a conductor could be calculated as in Eq. (2), by means of resistivity ρ, length l, and cross-sectional area S of the conductor.

$$R_{dc} = \ \frac{\rho.l}{S} \tag{2}$$

The skin effect coefficient y_s is given by

$$y_s = \frac{X_s^4}{192 + 0,8X_s^4} \tag{3}$$

where,

$$X_s = \ \sqrt{\frac{8\pi f}{R_{dc}} 10^{-7} k_p} \tag{4}$$

Similarly, the proximity effect coefficient y_p is given by

$$y_p = \frac{X_p^4}{192 + 0,8X_p^4} \quad \left(\frac{D_i}{a}\right)^2 .2,9 \tag{5}$$

and

$$X_p = \ \sqrt{\frac{8\pi f}{R_{dc}} 10^{-7} k_p} \tag{6}$$

where f is the supply frequency, D_i is the diameter of conductor, and a is the distance between conductor axes. Values for k_s and k_p are obtained from IEC 60287-1-1:2014 international standard [15].

These equations get more complicated in systems with large number of parallel cables. For this reason, computer software using various mathematical methods provides a significant advantage by offering solutions with high accuracy in a very short time in systems that include a large number of conductors.

Within the impedance matrix formed for conductors in multiconductor systems, a difference occurs in the values of the matrix elements due to the skin and proximity effects. As a result, an imbalance occurs in the current distribution between the conductors. The amount of this imbalance varies depending on the phase sequence of the conductors as well as the screen and armor properties of the cables.

3. Modeling of the analyzed cable and busbar system

The application examined in this study is a distribution system, which provides power from the double-secondary transformer to a power converter. The transformer used in this application is a three-phase, 34.5/2x0.4kV, 50Hz transformer with Dy11y11 connected windings. The rectifier fed from the secondary side of this transformer draws 2953A current per phase. In the current application, 9 parallel cables are used for each phase in each low voltage winding of the transformer. A total of 54 cables were used, 27 of which are in each secondary winding

of the transformer. Each cable used has a cross section of 240mm^2. The distance between the output terminals of the low voltage windings of the transformer and the input terminals of the converter is 10 m. The single line diagram of the application examined is shown in Figure 1.

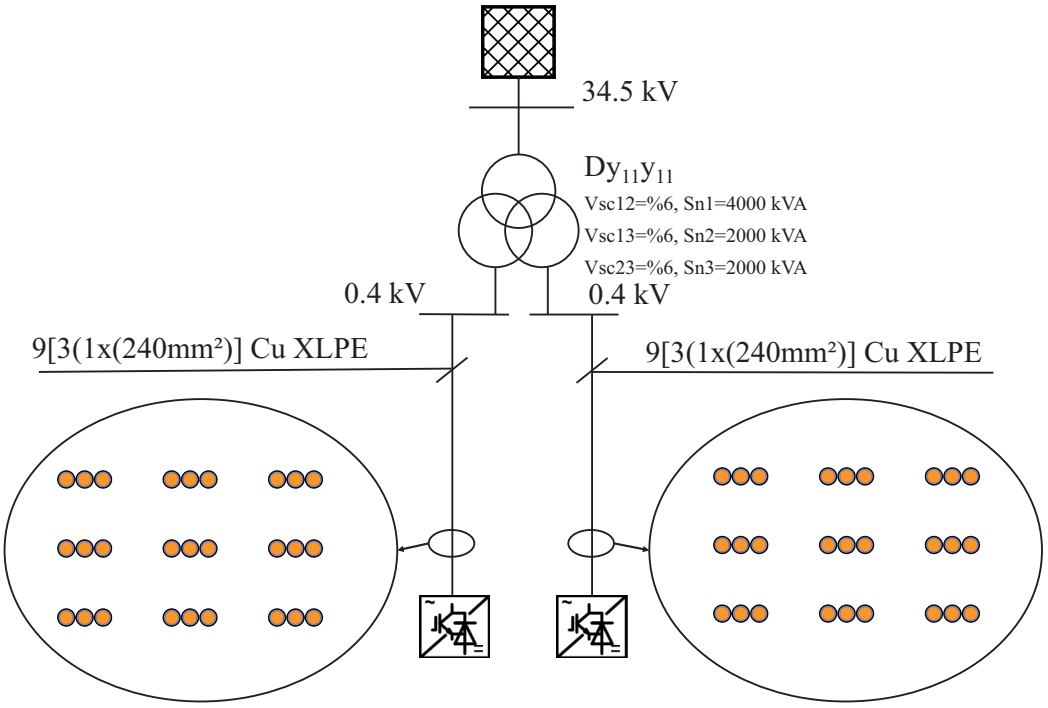

Figure 1. Single line diagram of the application.

In this study, it is aimed to compare both the current distribution in parallel conductors and the magnetic field values around the conductors in cases where the energy distribution on the secondary side of the transformer is provided using cable system or busbar system.

First, the existing cable application was modeled, and electromagnetic field analysis of this layout was performed. As a result, the current distributions on the conductors and the load imbalances between the parallel cables are determined. In addition, an analysis of electromagnetic field distributions occurring around cable layouts is performed.

Then, design and analysis are carried out for the case of performing the same application using busbars. The obtained results are compared with the cable system. For both applications, it is assumed that the current flowing through the conductors is pure sinusoidal and has no harmonic content.

Maxwell module of ANSYS Electronics Suite software, which provides a solution using finite element method, was used in the modeling and analysis stages of investigated cable and busbar systems. In cable and busbar models, the current carrying conductors of both systems are defined as copper material and the outer body of the busbar module as aluminum material. As the insulation material of the cables, XLPE and PVC material has been defined. The electrical conductivity and magnetic permeability values for these components are given in Table 1.

Table 1. Material parameters

Material	Place used	Electrical conductivity (S / m)	Relative permeability (H/m)
Annealed copper	Cable and bus conductor	58000000	0.999991
Aluminum	Busbar frame	36000000	1.000021
XLPE	Cable insulation	0	1
PVC	Cable cover	0	1

3.1. Cable system

In investigated application, each phase winding of each secondary circuit of the double-secondary transformer is connected to the rectifier using 9 parallel cables. Each of the cables has a 240 mm^2 cross section area and includes a copper conductor with XLPE insulation and has been installed as unarmored and unshielded. Physical and electrical properties for this cable are obtained from the manufacturer's catalogue[1] and are given in Table 2.

Table 2. Physical and electrical properties of the cable.

Cable parameters	Property
Cable type	N2XY 240 mm²
Current carrying capacity	750 A
Conductor diameter (copper)	18.1 mm
Insulation (XLPE)	21.5 mm
Cover (PVC)	25.1 mm
Resistance	0.075 Ω/km
Reactance	0.0795 Ω/km
Icw (1 sn)	34.32 kA

The phase sequence of 27 cables, which constitute each secondary circuit of the transformer, and their placement according to each other are shown in Figure 2. Accordingly, one cable of each phase is placed side by side with the L1, L2, L3 phase sequence to form a system. Establishing nine systems formed with this phase sequence as shown in Figure 2 , each secondary circuit of the transformer connected to the converter is formed.

Here, each cable is modeled with an impedance with its own resistance and self-inductance within the excitation circuit. The mutual inductance of the cables against each other is calculated by the software. The phase current with an effective value of 2953A is modeled with a sinusoidal current source and is applied to nine parallel systems. Phase currents applied to three phases are balanced and symmetrical, and there is also 120° phase difference between them.

The excitation circuit created for only one phase of each secondary circuit of the transformer in the electromagnetic simulation study is shown in Figure 3.

The current carrying capacity of the cable used in the application is given by the manufacturer as 750A for the installation of the cable in the air and operating temperature of 30° C. When calculated according to the reduction factors specified in the IEC 60364-5-52 standard, the total current carrying capacity for 9 parallel

[1]Has Celik Power Cables Product Catalog [online] Website http://kablo.hascelik.com.tr/online-katalog [accessed 26 January 2021]

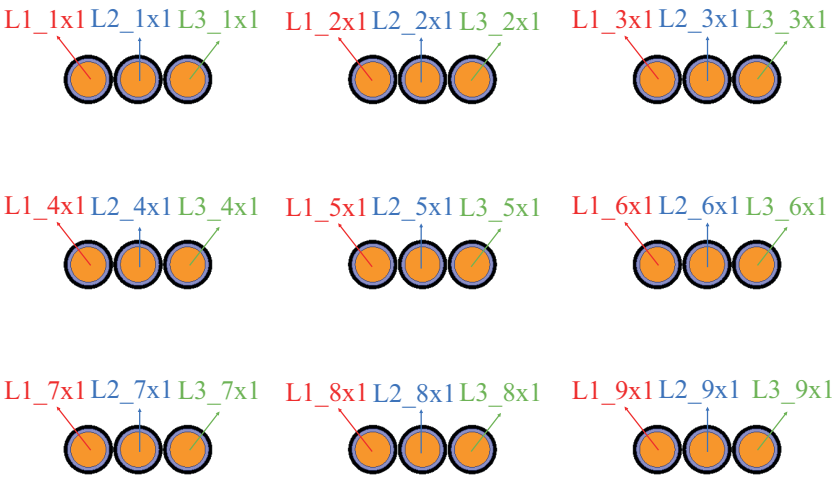

Figure 2. One secondary circuit of the transformer in cable structure.

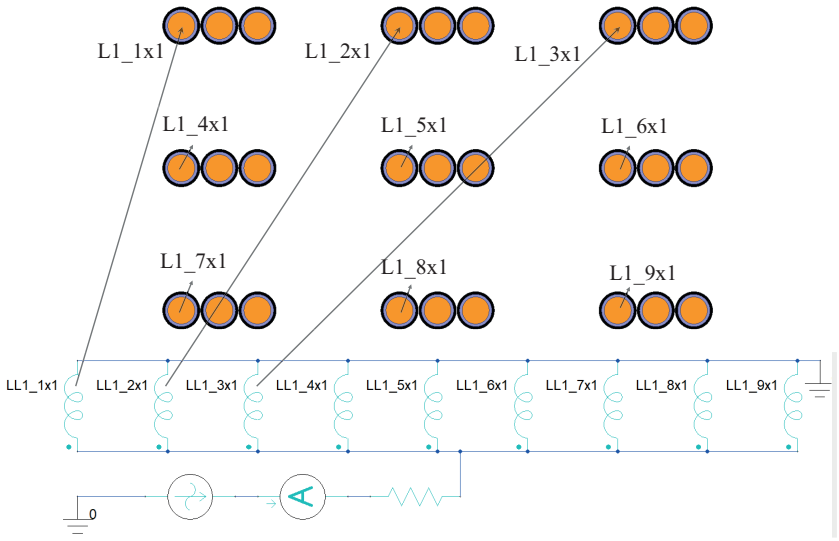

Figure 3. Excitation circuit of single phase of a secondary circuit in cable structure.

cables is obtained as 3375A [1]. Accordingly, it is seen that the existing cable layout in practice is suitable in terms of current carrying capacity.

3.2. Busbar system

The distribution system used in this studied application has been redesigned using the busbar structure to make various comparisons. All analyses have been made for the busbar structure to determine the current distribution between the conductors and the electromagnetic field that occurs around the conductors.

In this study, comparisons and evaluations are made for replacing the existing cable application with the commercially available busbar module structure. In the selection of the busbar module, the total cross-sectional area used in the cable system has been considered. The total conductor cross-sectional area of the cables with

9 pieces of 240mm^2 cross section per phase used in each secondary circuit of the cable application is calculated as 2160mm^2. The busbar type, closest to this cross-sectional area, has a cross-sectional area of 2400mm^2 per phase with a current carrying capacity of 5000A. For this reason, copper conductor EAE E-Line KX 5000 A CU busbar modules with a current carrying capacity of 5000A and a cross-sectional area of 2400mm^2 for one phase were used in each of the secondary circuits of the transformer.

The physical and electrical properties of the selected busbar are given in Table 3 [2].

Table 3. Physical and electrical properties of busbar.

Busbar parameters	Property
Conductor type	Copper
Current carrying capacity	5000 A
Conductor cross section	2400 mm^2
Body material	Aluminum (per phase)
Resistance	0.008 Ω/km
Reactance	0.004 Ω/km
Icw (1 sn)	120 kA

It is calculated that there is an approximate 11% difference between the conductor cross-section constituting one phase of the selected busbar module and the total conductor cross-section of 9 parallel cables forming a phase in the current application. Depending on the cross-section value, the conductor resistance and the power losses in the conductor are affected. Power losses and the effects of thermal conditions are not examined in this study. For this reason, it is not taken into account to use a correction factor to eliminate the effect of cross-sectional difference in the results obtained regarding the current distribution between parallel conductors.

In forming each secondary circuit of the transformer, two busbar modules are installed in parallel. Each busbar module has four copper conductors, three of which are phase conductors and one neutral conductor. The phase sequences and the locations of the busbar modules and conductors used in each secondary circuit are given in Figure 4.

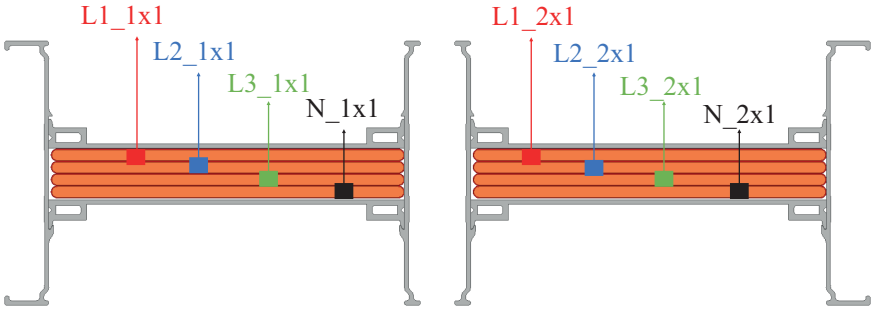

Figure 4. One secondary circuit of the transformer in busbar structure.

The excitation circuit created for only one phase of a secondary circuit of the transformer is shown in Figure 5. Each busbar conductor is modeled within the excitation circuit as an impedance with its own

[2]EAE Electric E-LINEKX Busbar Systems Product Catalog [online] Website https://www.eae.com.tr/pdf/eng/e-line-kx-en.pdf [accessed 26 February 2021]

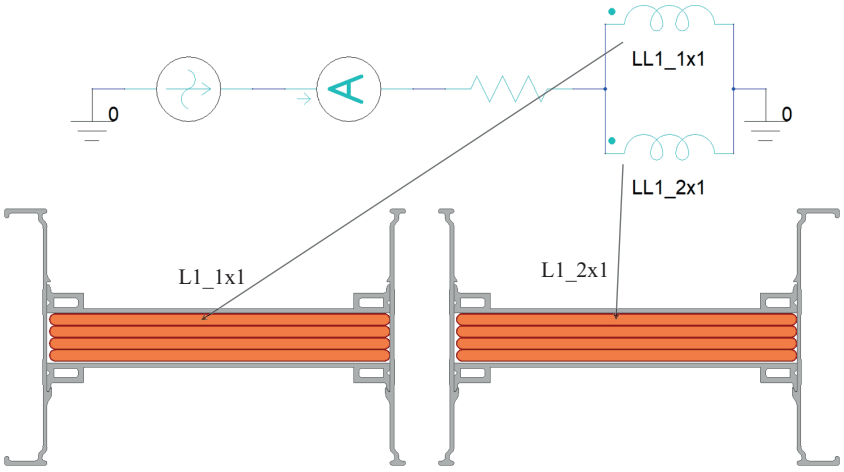

Figure 5. Excitation circuit of single phase of a secondary circuit in busbar structure.

resistance. The mutual inductance of the busbars against each other is calculated by the software. The phase current with an effective value of 2953A is modeled with a current source and is applied to two parallel busbar conductors. Phase currents applied to three phases are balanced and symmetrical, and there is also 120° phase difference between them.

4. Current distribution analysis

In the analysis, the conductor temperatures in the cable and busbar structure were accepted as 90°C, and the body temperature in the busbar structure as 50°C. The current waveform with 2953A effective value and 50 Hz frequency applied to phase conductors in all analyzes is shown in Figure 6.

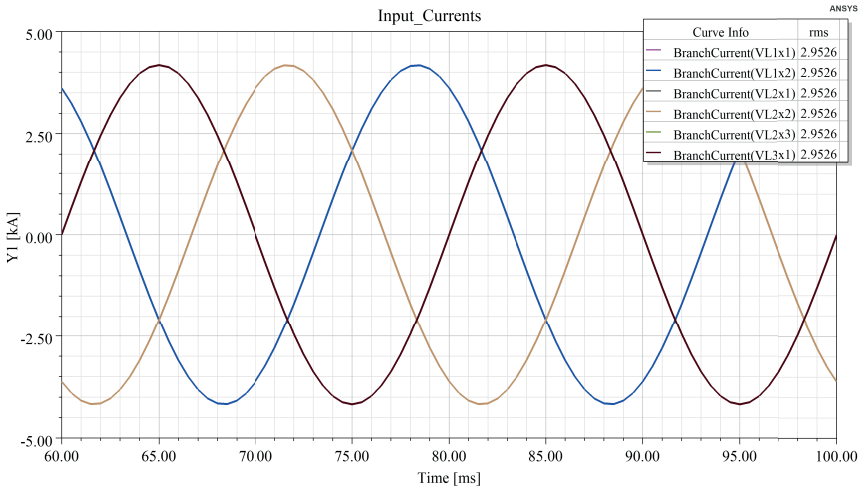

Figure 6. Applied current for cable and busbar systems during analysis studies.

4.1. Results of the current distribution on the cable system

The current flowing over each cable was determined with the analysis performed for the existing cable layout. As a result of the analysis studies, difference of the current values between secondary circuits is obtained in negligible level. Therefore, the calculated current values of parallel cables in only one circuit are given in Figure 7.

Calculated results show that the currents vary between 297.38A and 350.49A in a three-phase system, which corresponds to 17% imbalance between parallel cables. This difference mainly occurs due to the effect of mutual inductance between the conductors as well as skin and proximity effects. Amount of this difference depends on the factors such as the distance between cables, phase sequences, whether the cable shielded or not, whether the shield is grounded or not, etc. Analyzed cable system was modeled depending on the application as summarized in Figure 1.

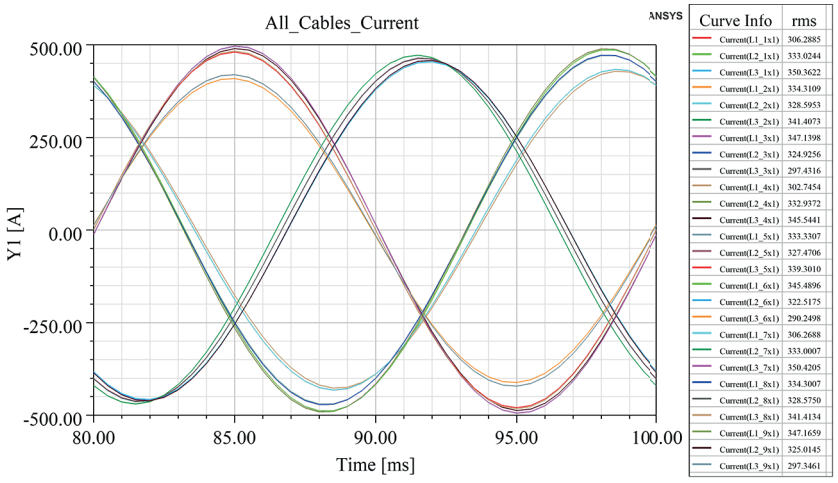

(a)

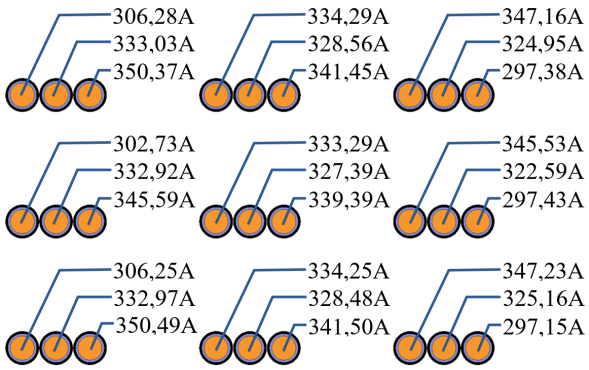

(b)

Figure 7. (a) Current waveforms. (b) Current distributions between parallel cables.

4.2. Results of the current distribution on the busbar system

As a result of the analysis studies, the current distribution between busbar conductors is shown in Figure 8. Obtained results show that the current imbalances calculated in cable application are not observed in the busbar structure. It is seen that the factors that create current imbalance in the cable system are not effective due to the fact that the design and analysis of the busbar structure consists of two parallel busbar modules, and these modules are located close to each other. The results show that the currents flowing from the phase conductors of the two parallel busbar modules used in each secondary circuit of the transformer are equally distributed.

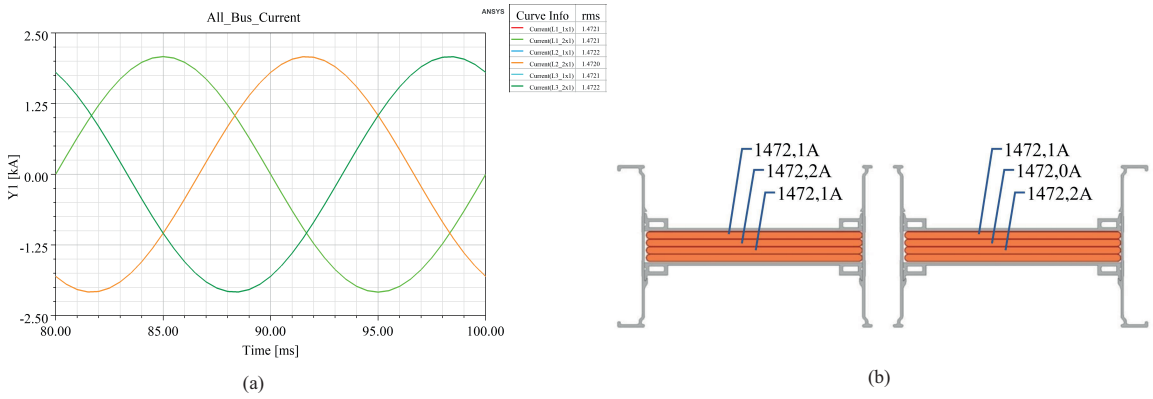

Figure 8. (a) Current waveforms. (b) Current distributions between parallel busbar conductors.

5. Electromagnetic field analysis

According to the Biot-Savart law, magnetic fields occur around current carrying conductors. In literature, it is stated that these magnetic fields have some negative effects on the health of human beings. To minimize these effects, limit values for electromagnetic fields have been determined and documented by ICNIRP. Accordingly, for the 50Hz network frequency, the highest magnetic field intensity values that can be encountered for public areas and occupational areas are specified as 0.2mT and 1mT, respectively [16]. In terms of human health, it is important not to exceed these limit values. In addition, electromagnetic fields have negative effects on electronic devices in working environments.

In this context, magnetic field analyzes were carried out in order to examine the magnetic field density values occurring around the conductors in cable and busbar structures.

In order to compare cable and busbar applications according to the same criteria, the method in IEC 61439-6 standard, which is used for experimental measurement of magnetic field values around busbar systems, has been simulated. Accordingly, magnetic field values were calculated at the points determined in five different measuring axes, namely A, B, C, D and E. In these calculations, IEC 62110 standard is taken into consideration for the cable system and IEC 61439-6 standard for the busbar system [17, 18].

According to these considered standards, the origin of the axis sets for both systems are placed in the middle of a secondary circuit of the models. Total measurement distance is defined as 750 mm, which starts from 450 mm distance to the axis origin and continues up to 1200 mm for five directions explained in Figure 9. Axis sets and the magnetic field distributions around cable and busbar systems are shown in Figure 10 and Figure 11.

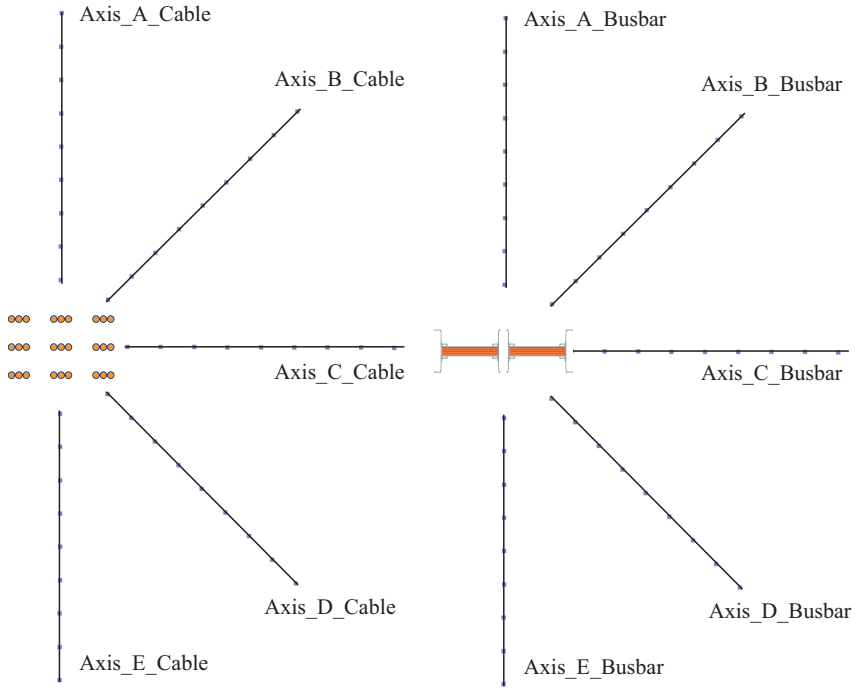

Figure 9. Analyzed axis system for cable and busbar model.

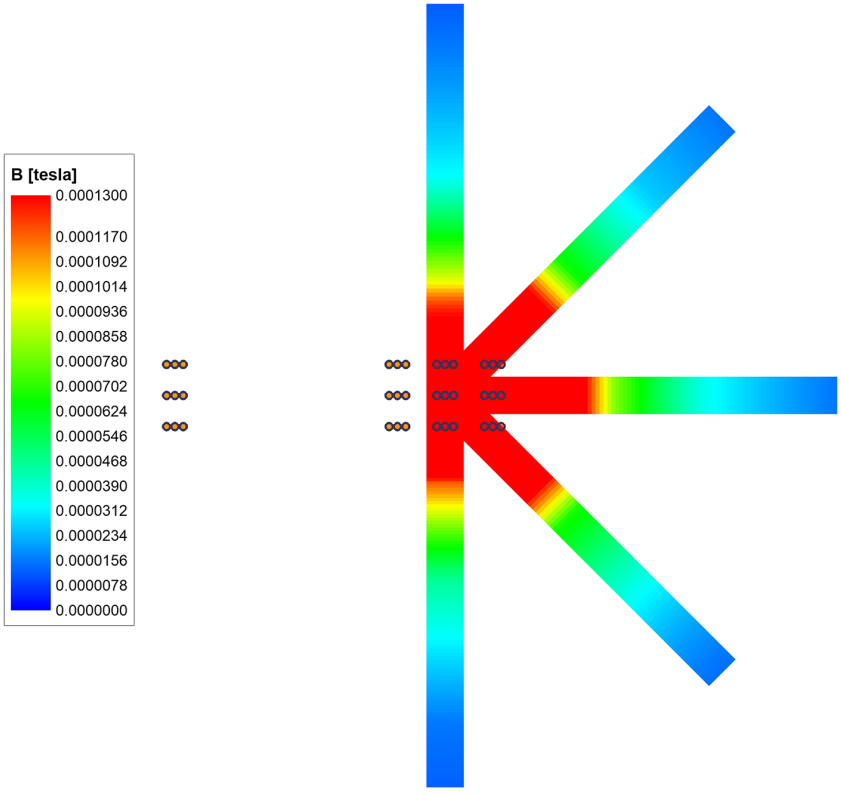

Figure 10. Magnetic field density distributions occurring on the axes for the cable system.

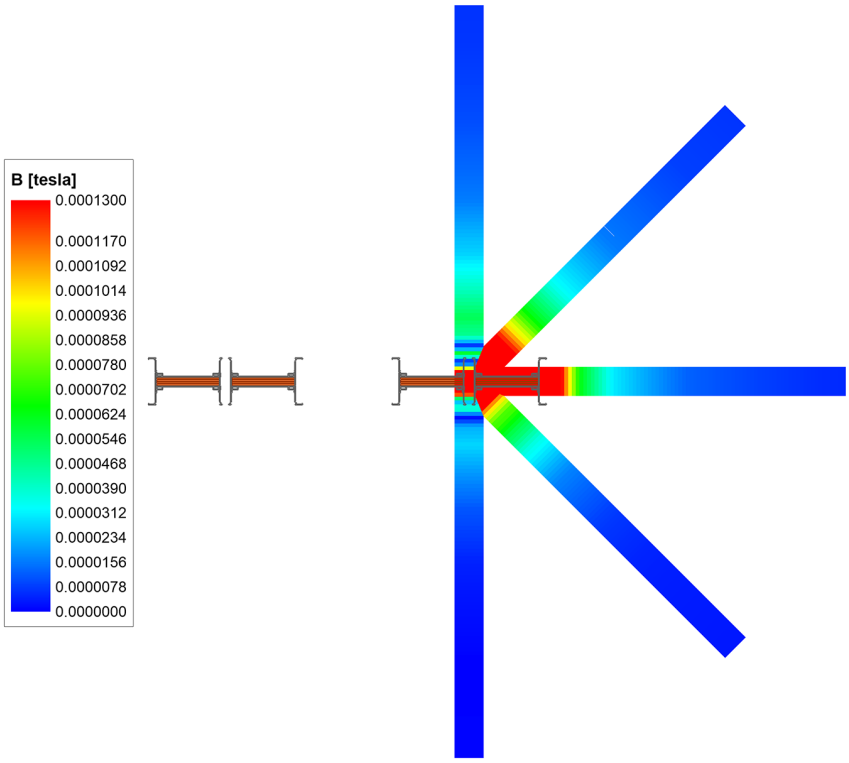

Figure 11. Magnetic field density distributions occurring on the axes for the busbar system.

In the analysis, the maximum density of the magnetic field occurring over a period was examined. Maximum magnetic field densities occurring on all axes are shown in Figure 12 depending on the axis distance for cable and busbar applications. In addition, it is assumed that there is no metal equipment that will affect the magnetic field distribution around the cable and busbar structure.

The maximum magnetic field density at 450 mm distance has obtained as 114 μT and 30 μT for the cable and busbar systems, respectively. Although the values obtained for both structures are within the allowed limits, it is seen that the highest magnetic field density value calculated for the cable structure is 3.8 times higher than the busbar structure.

The obtained values are directly related to the distance of the conductors in the modeled cable and busbar systems to the measurement points starting from 450 mm. As can be seen from Figure 9, the cable conductors that make up the cable structure are closer to the measuring distance starting from 450 mm, especially in the A, B, D and E axes, compared to the busbar conductors. This results in much higher magnetic field intensity over the entire measuring distance starting at 450 mm for the cable system without any shielding. For the busbar structure, in addition to the greater distance of the busbar conductors to the measuring distance, the aluminum body surrounding the busbar conductors undertakes the task of shielding and reduces the magnetic field intensity value formed around the busbar structure.

The magnetic field intensity value formed around the conductors decreases depending on the distance for cable and busbar structures. However, it can be clearly seen that, calculated maximum field density values for cable system are higher than the busbar structure in all directions.

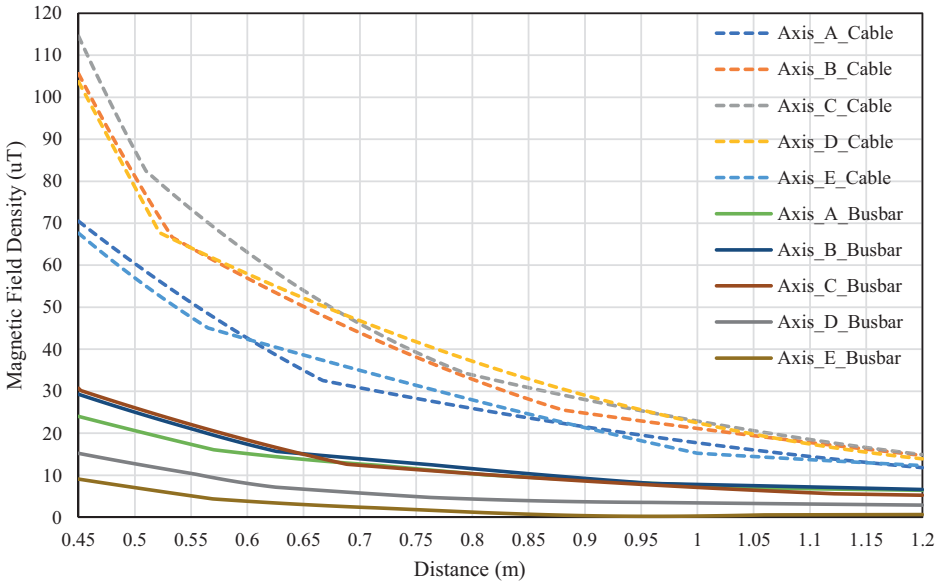

Figure 12. Maximum magnetic field densities occurring on all axes.

6. Conclusion

In this study, a comparison of parallel cable and busbar systems for low voltage power distribution application between a multi-winding transformer and a 12-pulse converter circuit is given.

Although power distribution with cable systems is widely carried out in energy systems, it is seen that the imbalance in current distribution between parallel conductors established especially in case of high current carrying reaches very high values when phase sequence, transpose, and shield grounding are not taken into consideration. In the performed analyzes for the application examined in this study, it was determined that the current imbalance between parallel cables was at the level of 17%.

For this application, the situation of power distribution with busbar system in accordance with the standards was evaluated and a design in this direction was realized. In the analyzes conducted for this design, it was determined that the current imbalance between the parallel busbar conductors is at a negligible level. This shows that the above-mentioned issues that should be considered for cable systems are no longer important.

In addition, magnetic field intensity values around the conductors for cable and busbar systems were investigated. Although results are similar to the studies in which busbars are examined in the literature, it is seen that the magnetic field density value around the conductors decreases by 73.7% compared to the cable application in case power distribution is carried out with busbar conductors.

Acknowledgment

The authors would like to thank to EAE Elektrik A.Ş. for their technical guidance and support.

References

[1] IEC. IEC TC 64. Low-voltage electrical installations - Part 5-52: Selection and erection of electrical equipment - Wiring systems. IEC Standard IEC 60364-5-52. Geneva, Switzerland: IEC, 2009.

[2] Lee SY. A cable configuration technique for the balance of current distribution in parallel cables. Journal of Marine Science and Technology 2010; 18 (2): 290-297.

[3] Wu AY. Single-Conductor Cables in Parallel. IEEE Transactions on Industry Applications 1984; IA-20 (2): 377-395. doi: 10.1109/TIA.1984.4504423

[4] Öztürk O, Karacasu Ö, Hocaoğlu M. Effects of parallel power cables on current distribution. In: National Conference on Electrical, Electronics and Computer Engineering; Bursa, Turkey; 2010. pp. 133-136.(article in Turkish with an abstract in English)

[5] Gouramanis K, Demoulias C. Cable overheating in an industrial substation feeder due to untransposed power cables - Measurement and simulation. In: The International Conference on "Computer as a Tool"; Belgrade, Serbia; 2005. pp. 1438-1441. doi: 10.1109/EURCON.2005.1630233

[6] Gouramanis K, Demoulias C, Labridis DP, Dokopoulos P. Distribution of non-sinusoidal currents in parallel conductors used in three-phase four-wire networks. Electric Power Systems Research 2009; 79 (5): 766-780. doi: 10.1016/j.epsr.2008.10.012

[7] Fernandez E. Cable arrangements for reduced magnetic field. Electrotechnik Pty. Ltd. Technical Report, pp. 1-5.

[8] Li Z, Zhong X, Xia J, Bian R, Xu S VRN et al. Simulation of current distribution in parallel single-core cables based on finite element method. In: 5th International Conference on Instrumentation and Measurement, Computer, Communication, and Control; Qinhuangdao, China; 2015. pp. 411-414. doi: 10.1109/IMCCC.2015.94

[9] Kadkhodaei G, Sheshyekani K, Hamzeh M, Tavakol SD. Multiphysics analysis of busbars with various arrangements under short-circuit condition. IET Electrical Systems in Transportation 2016; 6 (4): 237-245. doi: 10.1049/iet-est.2016.0043

[10] Jiaxin Y, Ruichao W, Huimin L, Longqing B, Hongjian W. Research on the calculation methods of enclosed isolated phase bus-bar in short-circuit condition. In: 2016 IEEE 62nd Holm Conference on Electrical Contacts (Holm); Clearwater Beach, FL, USA; 2016. pp. 111-114. doi: 10.1109/HOLM.2016.7780016

[11] Viswanatha C, Rakesh KG. Investigation of epoxy coated Busbar system enclosed in LT busduct of rating 2000A. In: 2016 IEEE 6th International Conference on Power Systems; New Delhi, India; 2016. pp. 1-5. doi: 10.1109/ICPES.2016.7584207

[12] Delgado F, Renedo C, Ortiz A, Fernandez I. Numerical model of a three-phase busbar trunking system. In: 2016 IEEE Electrical Insulation Conference; Montreal, QC, Canada; 2016. pp. 21-24. doi: 10.1109/EIC.2016.7548584.

[13] Voronin SV, Matantsev AN, Losses in Trunk Busbars. Russian Electrical Engineering 2018; 89 (6): 376-380. doi: 10.3103/S1068371218060111

[14] Popa IC, Dolan AI. Numerical modeling of three-phase busbar systems: Calculation of the thermal field and electrodynamic forces. In: 2016 International Conference on Applied and Theoretical Electricity; Craiova, Romania; 2016. pp. 1-9. doi: 10.1109/ICATE.2016.7754608

[15] IEC. IEC TC 20. Electric cables - Calculation of the current rating - Part 1-1: Current rating equations (100 % load factor) and calculation of losses - General. IEC Standard IEC 60287-1-1. Geneva, Switzerland: IEC, 2014.

[16] International Commission on Non-Ionizing Radiation Protection. ICNIRP Guidelines for limiting exposure to time-varying electric and magnetic fields (1Hz–100kHz). Healty Physics 2010; 99 (6): 818-836. doi: 10.1097/HP.0b013e3181f06c86

[17] IEC. IEC TC 106. Electric and magnetic field levels generated by AC power systems - Measurement procedures with regard to public exposure. IEC Standard IEC 62110. Geneva, Switzerland: IEC, 2009.

[18] IEC. IEC TC 65/SC 65C. Low-voltage switchgear and controlgear assemblies - Part 6: Busbar trunking systems (busways). IEC Standard IEC 62439-6. Geneva, Switzerland: IEC, 2010.